Infrared Spectroscopic and Mutational Studies on Putidaredoxin-Induced Conformational Changes in Ferrous CO-P450cam[†,‡]

Shingo Nagano,[*,#,$] Hideo Shimada,[*,#] Akiko Tarumi,[#] Takako Hishiki,[#] Yoko Kimata-Ariga,[#,⊥] Tsuyoshi Egawa,[#,||] Makoto Suematsu,[#] Sam-Yong Park,[§,+] Shin-ichi Adachi,[§] Yoshitsugu Shiro,[§] and Yuzuru Ishimura[#,&]

Department of Biochemistry and Integrative Medical Biology, School of Medicine, Keio University, 35 Shinano-machi, Shinjuku-ku, Tokyo 160-8582, Japan, and The Institute of Physical and Chemical Research (RIKEN), RIKEN Harima Institute, 1-1-1 Kouto, Mikazuki-cho, Sayo, Hyogo 679-5148, Japan

Received August 6, 2003; Revised Manuscript Received October 6, 2003

ABSTRACT: Ferrous-carbon monoxide bound form of cytochrome P450cam (CO-P450cam) has two infrared (IR) CO stretching bands at 1940 and 1932 cm^{-1}. The former band is dominant (>95% in area) for CO-P450cam free of putidaredoxin (Pdx), while the latter band is dominant (>95% in area) in the complex of CO-P450cam with reduced Pdx. The binding of Pdx to CO-P450cam thus evokes a conformational change in the heme active site. To study the mechanism involved in the conformational change, surface amino acid residues Arg79, Arg109, and Arg112 in P450cam were replaced with Lys, Gln, and Met. IR spectroscopic and kinetic analyses of the mutants revealed that an enzyme that has a larger 1932 cm^{-1} band area upon Pdx-binding has a larger catalytic activity. Examination of the crystal structures of R109K and R112K suggested that the interaction between the guanidium group of Arg112 and Pdx is important for the conformational change. The mutations did not change a coupling ratio between the hydroxylation product and oxygen consumed. We interpret these findings to mean that the interaction of P450cam with Pdx through Arg112 enhances electron donation from the proximal ligand (Cys357) to the O−O bond of iron-bound O_2 and, possibly, promotes electron transfer from reduced Pdx to oxyP450cam, thereby facilitating the O−O bond splitting.

Cytochrome P450cam (P450cam)[1] is a heme-containing monooxygenase that catalyzes the hydroxylation of D-camphor in *Pseudomonas putida* (*1*, *2*). The ferric D-camphor-free enzyme first binds D-camphor to give the ferric D-camphor-bound state. This substrate-bound form then accepts one electron from reduced putidaredoxin (Pdx), yielding a substrate-bound ferrous form. Subsequent binding of O_2 to the ferrous form produces a D-camphor-bound ferrous-O_2 derivative (oxyP450cam). Upon a second one-electron reduction by Pdx, the oxyP450cam derivative proceeds to the D-camphor hydroxylation reaction, yielding 5-*exo*-hydroxycamphor and water and regenerating the ferric substrate-free resting state. Two protons are required for this reaction and are delivered into the active site of the enzyme through a proton delivery system (*3*−*7*).

Two redox-linked proteins, a flavoprotein putidaredoxin reductase (PdR) and an iron−sulfur protein Pdx, are necessary for transfer of two electrons from NADH to P450cam (*1*, *2*). On the other hand, other iron−sulfur proteins such as spinach ferredoxin and beef adrenodoxin readily provide the first electron but not the second one to support the D-camphor hydroxylation (*8*). On the basis of these and other findings, Lipscomb et al. proposed that, in addition to be an electron shuttle, Pdx plays a role as an "effector" in the D-camphor monooxygenation reaction. Since then, various spectroscopic studies including NMR (*9*−*11*), EPR (*12*), IR (*13*), and resonance Raman (*14*, *15*) have been carried out to examine the interaction between P450cam and Pdx. The

[†] This work was supported in part by grants-in-aid for scientific research on priority areas, scientific research (C), and the 21st Century Center of Excellence (COE) Program Entitled "Understanding and Control of Life's Function via Systems Biology (Keio University)" from Ministry of Education, Science, Culture, Sports and Technology of Japan and by grants from Keio University.

[‡] The structural coordinates and the structure factors are deposited in the Protein Data Bank under accession codes 1IWI, 1IWJ, and 1IWK for ferric D-camphor bound forms of wild-type P450cam, R109K, and R112K mutants, respectively.

* To whom correspondence should be addressed. E-mail: shimada@sc.itc.keio.ac.jp; fax: 81−3−3358−8138; phone: 81−3−3353−1997. E-mail: snagano@uci.edu; fax: 1−949−824−3280; phone: 1−949−824−4322

[#] Keio University.

[§] RIKEN Harima Institute.

[$] Present address: Department of Molecular Biology and Biochemistry and the Program in Macromolecular Structure, University of California, Irvine, Irvine CA 92697-3900 USA.

[⊥] Present address: Division of Enzymology, Institute for Protein Research, Osaka University, Yamadaoka 3−2, Suita, Osaka 565-0871, Japan.

[+] Present address: Protein Design Laboratory, Graduate School of Integrated Science, Yokohama City University, 1−7−29 Suehiro-cho, Tsurumi, Yokohama 230-0045, Japan.

[&] Present address: Department of Biochemistry, The University of Texas Health Science Center at San Antonio, San Antonio, TX 78229-3900, USA.

[||] Present address: Department of Biochemistry and Biophysics, University of Pennsylvania.

[1] Abbreviations: P450cam, cytochrome P450 (CYP101) originally isolated from *Pseudomonas putida*. It catalyzes the conversion of D-camphor to 5-*exo*-hydroxycamphor; PdR, putidaredoxin reductase; Pdx, putidaredoxin; oxyP450cam, D-camphor-bound ferrous-O_2 P450cam; CO-P450cam, D-camphor-bound ferrous-carbon monoxide P450cam, IR; infrared, EPR; electron paramagnetic resonance.

10.1021/bi035410p CCC: $25.00
Published on Web 11/19/2003

Table 1: Kinetic and Spectroscopic Properties of Wild-Type P450cam and Its Mutants

protein	O_2 consumption rate (μM min^{-1} (μM enzyme)$^{-1}$)	coupling ratio[a] (%)	k_2[b] (s^{-1})	band II intensity[c] (arbitrary unit)	K_d^{IR} (μM)[d]	K_d^{kin} (μM)[e]
WT	1400 (100%)	100	169	0.97 ± 0.09	22	12
R109K	500 (36%)	100	126	0.18 ± 0.06	79	47
R109Q	100 (7%)	100	66	0.09 ± 0.09	916	208
R112K	200 (14%)	88	87	0.16 ± 0.02	38	76
R79Q	1480 (106%)	100	N.D.[f]	*g*	N.D.[f]	N.D.[f]
R112M	1.7 (0.1%)[h]	86[h]	*i*	*j*	N.D.[f]	N.D.[f]

[a] Ratio between the hydroxylated product (5-*exo*-hydroxy camphor) and O_2 consumed. [b] Apparent rate constants for breakdown of oxyP450cam/Pdx complex. [c] Band II area of CO-P450cam/Pdx complex relative to the whole band area. Data are mean ± standard deviation. [d] Apparent dissociation constants calculated from IR titration. [e] Apparent dissociation constants calculated from kinetic analysis of breakdown of oxyP450cam/Pdx complex. [f] Not determined. [g] Addition of 5-fold excess amount of reduced Pdx gives almost identical spectrum of wild-type CO-P450cam/Pdx complex. [h] Data from Unno et al. (*20*). [i] OxyR112M in the presence of 200-fold excess of reduced Pdx does not decay over 500 ms. [j] No significant ν_{CO} spectral change was observed even when 20-fold excess of reduced Pdx was added.

results have established unambiguously that Pdx binding produces significant changes in the structure of the heme active center in P450cam. However, the molecular mechanism by which the conformational change occurs and the significance of the conformational change remain unclear.

In the present study, we examined effects of mutation at the presumed Pdx-binding site of P450cam on the conformational change as well as the catalytic properties of P450cam; Arg79, Arg109, Arg112 are the residues in the presumed Pdx binding site (*16*). Among them, Arg109 and Arg112 mutants showed significantly decreased catalytic activities together with decreased binding affinities to Pdx. X-ray crystallographic and IR spectroscopic studies indicated that the overall structures of 109 and 112 mutants are not eminently different from that of the wild-type P450cam. However, both mutants exhibited much less conformational conversion than that occurring in the wild-type P450cam upon complex formation with Pdx, presumably due to the lack of hydrogen bonding between Arg112 and Pdx. On the basis of these results, the molecular mechanism and functional significance of the conformational change are discussed.

EXPERIMENTAL PROCEDURES

Enzyme Purification and Assay. The mutagenesis of the P450cam gene was performed as previously described (*5*, *17*). The wild-type P450cam and its mutants were expressed in *Escherichia coli* strain JM109 and purified according to the procedures described previously (*18*). Purified P450cam with an *RZ* value (A_{391}/A_{280}) greater than 1.5 was used in this study unless otherwise stated. Pdx and PdR were also expressed in *Escherichia coli* strain JM109 and were purified to a homogeneous state according to the methods described by Gunsalus and Wagner (*19*). Catalytic activity of P450cam was determined by measuring simultaneously oxygen consumption and NADH oxidation at 20 °C in a reconstituted system composed of 360 μM NADH, 14 μM Pdx, 0.12 μM PdR, and an appropriate amount of P450cam in 50 mM potassium phosphate, pH7.4, containing 50 mM KCl and 1 mM D-camphor (hereafter designated buffer A) (*5*, *18*). The activity of the wild-type P450cam and its mutants, R79Q, R109K, R109Q, and R112K was measured in this work and presented in Table 1, while that of R112M was presented elsewhere (*20*).

The rates for degradation of oxyP450cam into ferric enzyme and 5-*exo*-hydroxycamphor upon reaction with reduced Pdx were measured at 4 °C by monitoring the spectral changes of oxyP450cam from 380 to 540 nm on a Unisoku stopped-flow/rapid-scan spectrophotometer, model RSP-601 (Osaka, Japan) as described previously (*5*). The reaction between oxyP450cam and reduced Pdx is shown as follows:

$$A + B \rightleftarrows C \xrightarrow{k_2} D$$

In this reaction scheme, species A and B represent oxyP450cam and reduced Pdx, respectively. Species C shows the oxyP450cam/Pdx complex and D represents the product proteins, ferric P450cam and oxidized Pdx. The bimolecular association is, as shown in the previous study (*21*), sufficiently faster than the breakdown of the oxyP450cam/Pdx complex. An excess amount of Pdx over P450cam was used for this experiment. In such a case, the observed rate constants (k_{obs}) are expressed as eq i (*22*)

$$k_{obs} = k_2[\mathrm{Pdx}]/(K_d^{kin} + [\mathrm{Pdx}]) \quad \text{(i)}$$

where k_2 is the apparent rate constant for the breakdown of the oxyP450cam/Pdx complex, K_d^{kin} is the apparent dissociation constant for the oxyP450cam/Pdx complex, and [Pdx] is the initial concentration of reduced Pdx, which is sufficiently larger than the P450cam concentration.

Measurement of IR ν_{C-O} Spectra. CO-P450cam was prepared as follows: 80−100 μL of P450cam or a mixture of P450cam and Pdx in buffer A in a 3-mL vial sealed with a vaccine cap was made anaerobic by passing N_2 gas into the vial through the vaccine cap. Then sodium dithionite in alkaline buffer was added to reduce the protein. After reduction of the sample, the atmosphere of the vial was changed to CO using the procedure described above. The protein was anaerobically transferred to an IR cell (Specac, England) with 0.05-mm path length CaF_2 windows. IR spectra were measured at 20 °C with a PerkinElmer FT-IR spectrophotometer, system 2000 (Buckinghamshire, England) with an Hg/Cd/Te detector. A 1000 scan interferogram was collected in a single beam mode with 2 cm^{-1} resolution. Buffer A spectra obtained under identical conditions were used as reference spectra. UV−visible absorption spectra were measured before and after IR spectral measurements and no difference was found. A baseline of the spectra was corrected with a cubic spline function.

Analysis of IR Spectra. IR ν_{C-O} spectra of CO-P450cam were decomposed into single bands of Gaussian shape (*23*,

Table 2: Data Collection and Structure Refinement Statistics and Crystal Parameters

data set	wild type	R109K	R112K
resolution range (Å)	15.0−2.0	15.0−2.0	20.0−2.0
unit cell dimensions (Å)	$a = 109.12$ $b = 104.33$ $c = 36.18$	$a = 109.16$ $b = 104.33$ $c = 36.14$	$a = 104.18$ $b = 104.13$ $c = 36.65$
reflections measured/unique	163,126/27,250	118,057/27,413	158,280/25,273
completeness overall/outer shell (2.11−2.00)	95.1/79.8	95.1/79.8	88.4/67.4
R_{merge} (%)[a] overall/outer shell (2.11−2.00)	3.2/6.1	3.3/5.4	9.0/41.3
redundancy	3.9	3.2	4.3
Refinement Statistics			
resolution range (Å)	15.0−2.0	15.0−2.0	20.0−2.0
σ cutoff	0.0	0.0	0.0
reflections used	27,215	27,370	24,998
R factor (%)[b]	17.3	16.6	17.9
R_{free} factor (%)[b]	22.9	22.1	23.2
no. of water molecules	187	180	175
RMS deviations from ideal			
bond length (Å)	0.007	0.007	0.006
bond angles (degree)	1.134	1.129	1.126
Ramachandran plot			
residues in most favorable regions (%)	91.1	91.1	90.8
residues in favorable regions (%)	8.9	8.9	9.2
residues in disallowed regions (%)	0.0	0.0	0.0

[a] $R_{merge} = \Sigma |I_i - \langle I \rangle| / \Sigma |I_i|$, where I_i is the intensity of an observation and $\langle I \rangle$ is the mean value for that reflection and the summations are overall reflections. [b] R factor $= \Sigma_h ||F_o(h)| - |F_c(h)|| / \Sigma_h |F_o(h)|$, where F_o and F_c are the observed and calculated structure factor amplitudes, respectively. R_{free} factor was calculated with 5% of the data.

24) with a minimal number of bands to obtain flat residuals (the differences between the observed and sums of componental bands). The decomposition was performed by using a multipeak fitting function of IgorPro software (WaveMetrics, Inc., Lake Oswego, OR). When Pdx-binding induced spectral changes were analyzed, the area of each componental band at the end point of titration and dissociation constants (K_d^{IR}) were determined by fitting the data using a least-squares minimization procedure of an equation corresponding to reversible binding of a 1:1 complex.

$$\Delta S = \Delta S_\infty \{L + K_d^{IR} + E - [(L + K_d^{IR} + E)^2 - 4EL]\}^{1/2}/2E \quad \text{(ii)}$$

In this equation, ΔS is the change in componental band area for a total Pdx concentration L. ΔS_∞ is the maximum change of componental band area, and E is the total P450cam concentration.

Crystallization and X-ray Crystallography. R109K and R112K mutants of P450cam were crystallized according to previously published procedures (*5*, *25*) and the X-ray crystallographic analysis was performed as described previously (*5*). P450cam samples with an *RZ* higher than 1.6 were employed for the crystallization. The data collection and refinement statistics and crystal parameters are given in Table 2.

RESULTS

Catalytic Activities. The catalytic activities of the wild-type enzyme and all mutant enzymes were measured as described under Experimental Procedures. The oxygen consumption rates and coupling ratios of oxygen consumption to the D-camphor monooxygenation (5-*exo*-hydroxycamphor/O_2 consumed in %) are listed in Table 1. The mutations of Arg109 and Arg112 at the presumed Pdx-binding site reduce the O_2 consumption rate to less than 40% of the wild-type enzyme. The values for R112K mutant were in good agreement with the previously reported values (*20*). The mutation at Arg79 had no effect on the enzymatic activities to wild type, suggesting that this residue is not important for activity. Although all the 109 and 112 mutants of P450cam investigated herein exhibit reduced oxygen consumption activities, they all catalyze the monooxygenation of D-camphor with a good coupling ratio (86−100%), indicating that oxyP450cam decomposes stoichiometrically into ferric P450cam, H_2O, and 5-*exo*-hydroxycamphor. This phenomenon is in contrast with the case of the Ala mutation at Thr252, which reduces the coupling ratio to 6% (*18*).

Reaction of oxyP450cam with Reduced Pdx. We next measured rates of decomposition of oxyP450cam with reduced Pdx for wild-type and mutant enzymes. Figure 1A,B shows time courses of the reactions of reduced Pdx with wild type and R112K, respectively. As shown, the experimental data fitted well to a single-exponential curve as reported previously for the wild-type enzyme (*20*). Time courses of the reaction catalyzed by wild-type P450cam as well as by its mutants always followed the first-order kinetics under different Pdx concentrations. Figure 2 shows plots of apparent first-order rate constant (k_{obs}) as a function of Pdx concentration. Rate constants (k_2) for breakdown of the

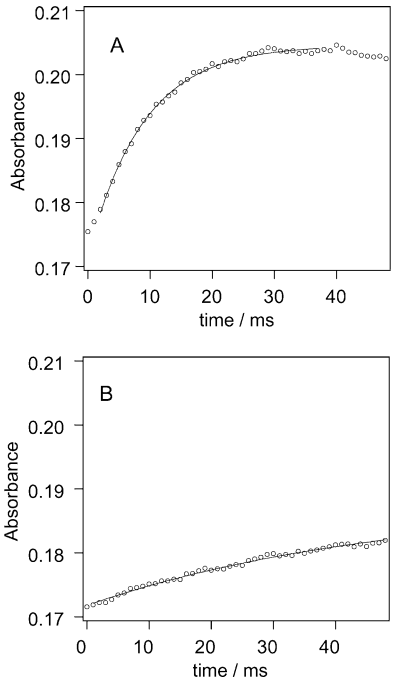

FIGURE 1: Stopped-flow analysis of the reaction between oxyP450cam and reduced Pdx. The reaction was followed by monitoring the changes in absorbance at 420 nm of P450cam after mixing oxyP450cam with reduced Pdx. Panel A represents the data for wild type, and panel B represents the data for R109K. The final concentrations of the reaction components after mixing were as follows: [P450cam] = 1.0 μM, [Pdx] = 10 μM, [metyrapone] = 5 mM. The reaction was performed at 4 °C in 50 mM K phosphate buffer, pH 7.4, containing 50 mM KCl and 1 mM D-camphor. The solid line through the experimental data points represents a single exponential fit to the data. OxyP450cam and reduced Pdx were prepared as described previously (*5*).

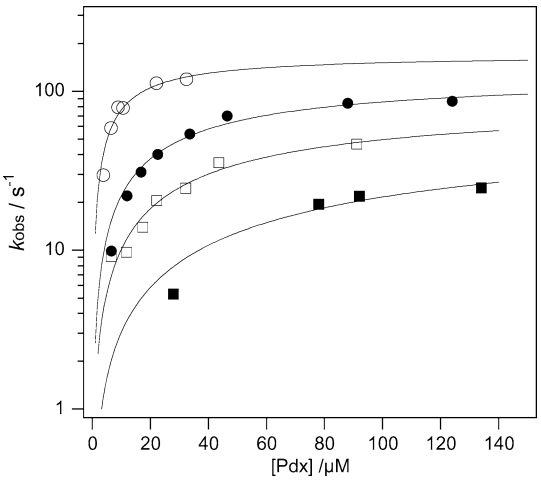

FIGURE 2: Observed rate constant (k_{obs}) for the reaction of oxyP450cam in the presence of a varying concentration of reduced Pdx. Rate constants were obtained from a single-exponential fitting to the time course data of the reaction such as those shown in Figure 1. k_{obs} values are shown for wild type (open circle), R109K (closed circle), R112K (open square), R109Q (closed square). The reaction was performed at 4 °C in 50 mM K phosphate, pH 7.4, containing 50 mM KCl and 1 mM D-camphor. Initial oxyP450cam concentration was fixed at 1.0 μM.

complex formed between oxyP450cam and Pdx and apparent dissociation constants (K_d^{kin}) of oxyP450cam/reduced Pdx complex were obtained from curve fitting of the eq i to the experimental data (Table 1). k_{obs} for the wild-type enzyme was larger than that for the mutants over the whole range of

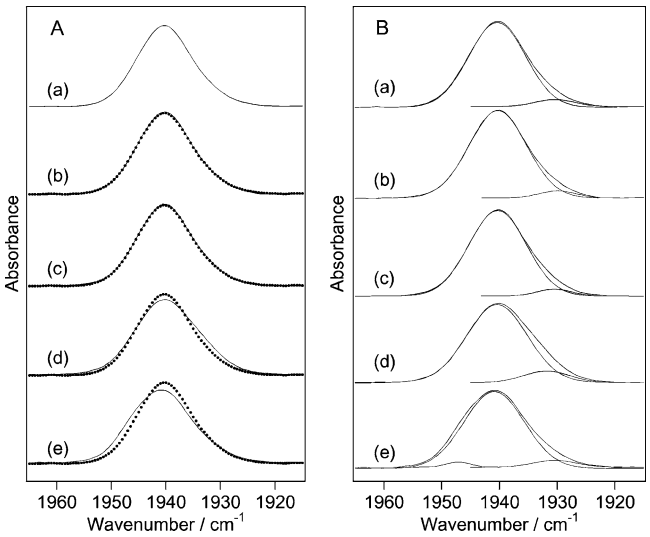

FIGURE 3: IR ν_{C-O} spectra of CO-P450cam of wild type and mutants. The spectra are 500 μM P450cam in 50 mM K phosphate buffer, pH 7.4, containing 50 mM KCl and 1 mM D-camphor and 20 °C. Traces in panel A and B are of wild type (a), R109K (b), R109Q (c), R112K (d), and R112M (e). In panel A, the wild-type spectrum is shown as dotted lines in traces b−e. Panel B shows decomposed single spectra for each spectrum. CO-P450cam was prepared as described in Experimental Procedures.

Pdx concentration examined and k_{obs} for the mutants were R109K > R112K > R109Q. In each profile, the rate constant reaches a plateau as the concentration of Pdx exceeds 20 μM for the wild-type P450cam and 80 μM for the three mutants. It is of note that R112M oxyP450cam did not decompose in the presence of 200-fold excess of reduced Pdx for over 500 ms, suggesting that the observed rate constants (k_{obs}) for R112M were less than 1% of the wild type in the whole Pdx concentration range examined. Thus, the introduction of neutral side chain at 112 drastically retarded the rate of breakdown of its oxy form. That the mutations at position 112 significantly reduced the rate for breakdown of the oxyP450cam with Pdx and its affinity for Pdx indicated that Ag112 is a critical residue required for P450cam−Pdx interaction and the monooxygenation reaction. In addition, Arg109 also turned out to be a critical residue. From the present and previous results (*20*, *26*, *27*), we conclude that Arg109 and Arg112 are the constituents of the Pdx-binding site for oxy-ferrous and ferric states of P450cam.

IR ν_{C-O} Spectra. We measured IR ν_{C-O} spectra of CO-P450cam in the absence and presence of reduced Pdx, as a stable mimic of oxyP450cam. Spectra of the wild-type enzyme and its mutant in the absence of Pdx are shown in Figure 3. The spectrum of the wild-type P450cam (trace a in Figure 3A) exhibits an almost symmetric ν_{C-O} band at 1940 cm^{-1} as reported previously (*13*, *28*, *29*). Decomposition of the spectrum into single bands revealed that, in addition to the main band at 1940 cm^{-1}, a minor band at 1932 cm^{-1} was present in the spectrum of the wild-type enzyme (trace a in Figure 3B). The main and minor bands (bands I and II, respectively) account for 95 and 5% of the entire band area. The spectra of R79Q, R109K, and R109Q mutant P450cam were almost identical to that of the wild-type enzyme (traces b and c in Figure 3A; spectrum for R79Q not shown). Decomposition of these mutant spectra also yielded two bands with the same band area and frequencies

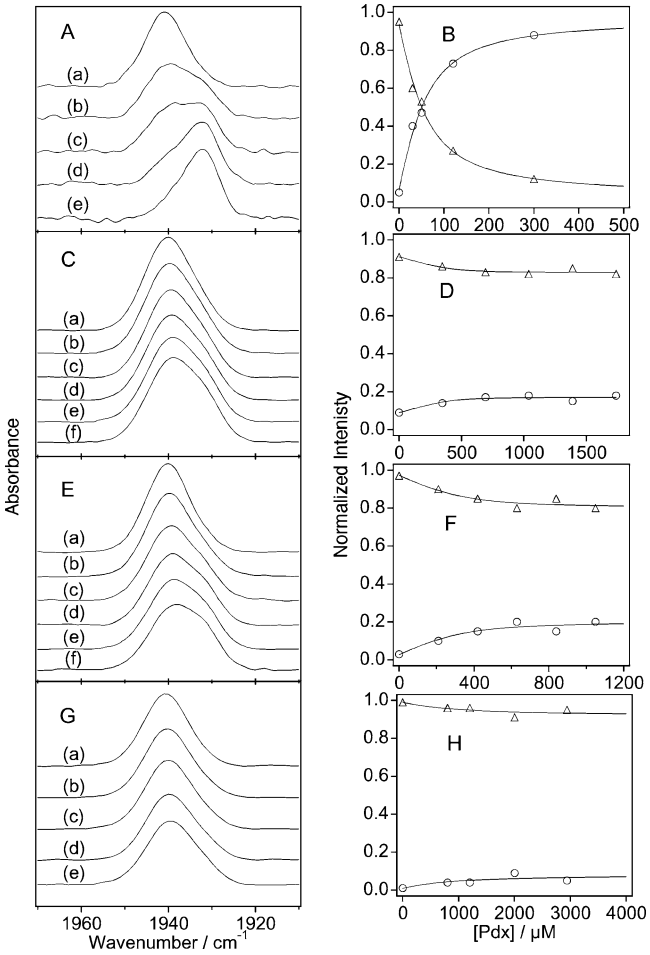

FIGURE 4: IR ν_{C-O} spectra of CO-P450cam in the presence of a varying concentration of reduced Pdx. (A) 45 μM wild-type P450cam and [Pdx] = 0 (a), 30 (b), 50 (c), 120 (d), and 300 μM (e). (C) 420 μM R112K and [Pdx] = 0 (a), 350 (b), 690 (c), 1040 (d), 1390 (e), and 1740 μM (f). (E) 320 μM R109K and [Pdx] = 0 (a), 210 (b), 420 (c), 630 (d), 840 (e), and 1050 μM (f). (G) 320 μM R109Q and [Pdx] = 0 (a), 800 (b), 1200 (c), 2000 (d), and 2940 μM (e). Changes in bands I (open triangle) and II (open circle) intensities vs [Pdx] are presented in panels B, D, F, and H for wild type, R112K, R109K, and R109Q, respectively. The other measurement conditions are as indicated for Figure 3.

as found for the wild type (traces b and c in Figure 3B; spectrum for R79Q is not shown), indicating that the mutations had little effect on the IR spectra. The mutation of Arg112 to Lys caused a slight reduction of the intensity of band I while causing a subtle broadening at the lower energy side of the band as shown in trace d of Figure 3A. These small changes were ascribed to changes in areas of bands I and II to 90 and 10%, respectively, without shifting the frequencies (trace d in Figure 3B). The R112M mutant shows more changes (trace e in Figure 3A). In addition to the bands I and II (band area = 90 and 7%, respectively), the spectrum exhibited an extra band at 1947 cm^{-1} (band area = 3%) (spectrum e in Figure 3B).

Next, we measured IR ν_{C-O} spectra of CO-P450cam in the presence of a varying concentration of Pdx. Wild-type P450cam showed spectral changes as the concentration of Pdx was raised as shown in Figure 4A. In the presence of about 3 equiv of Pdx and more, its ν_{C-O} changed to an asymmetric band centered at 1932 cm^{-1} (traces d and e in Figure 4A). Decomposition of these spectra revealed that band I decreased as the concentration of Pdx increased with a concomitant increase of band II, although the band frequencies did not shift. The areas of bands I and II were plotted as a function of Pdx concentration (Figure 4B). From the best-fitted titration curve obtained by assuming a 1:1 complex, wild-type CO-P450cam was shown to have bands I and II, which have relative intensities of 3 and 97%, respectively. The dissociation constant (K_d^{IR}) of the wild-type P450cam for reduced Pdx was determined to be 22 μM, which is in good agreement with the value derived from NMR titration (*10*, *11*) and that from current kinetic analysis (K_d^{kin} in Table 1). Decomposition of R112K spectra (Figure 4D) also revealed that band II intensity increased while band I decreased as Pdx concentration was raised. However, the change is remarkably small compared with that of the wild type (Figure 4B): CO-P450cam/Pdx complex of R112K exhibited bands I and II with relative band intensities of 80 and 20%, respectively. Analysis of the profile of the band intensity vs [Pdx] revealed that the dissociation constant of the R112K was 38 μM (Table 1). Likewise, both R109K and R109Q mutants had a less intense band II in the CO-P450cam/Pdx complex and had larger K_d^{IR} values than wild-type enzyme (Figure 4E−H and Table 1). R112M mutant showed little spectral change even in the presence of 20 equiv of reduced Pdx (spectra not shown). Hence, although all the 109 and 112 mutations decreased the binding affinity of P450cam to reduced Pdx, their most prominent effect was the remarkable decrease of the conformational change at the active site resulting from Pdx binding.

X-ray Crystal Structures. To gain further insight into the effects of mutations on the interaction between Pdx and P450cam, we analyzed the X-ray crystal structures of the wild-type, R109K, and R112K mutant enzymes at 2.0-Å resolution (Table 2 and Figure 5). The two mutant enzyme structures have overall root-mean-square differences of 0.06 and 0.16 Å, respectively, in main chain atoms from the wild-type enzyme. Such small root-mean-square differences indicate that the overall structures of the mutant proteins are essentially identical to that of the wild-type enzyme. The distal side structure including D-camphor and Thr252, which is a critical residue for a proton supply leading to O−O bond scission (*3*−*7*), is essentially unchanged by the mutations (Figure 5B,C). As found for wild type, Lys109 is projected outward away from the surface of the molecule. The R109K mutation caused no significant change at the proximal side structure. In contrast, the R112K mutation significantly altered the conformation of the loop including the proximal ligand: the backbone atoms of Leu358 moved toward the heme by 0.6 Å.

DISCUSSION

Conformational Change and Breakdown of oxyP450cam. To date, numerous spectroscopic studies have been carried out to elucidate the role of conformational changes on P450cam induced by Pdx binding. However, no quantitative evaluations have been made in terms of the relationship between the conformational changes and oxygen activation of P450cam. Current IR spectroscopic and kinetic data provide significant insight into this relationship.

Mutations at 109 and 112 notably changed intensity distribution of bands I and II of the CO-P450cam/Pdx complex. Relative band II intensities are 97, 18, 16, and 9%

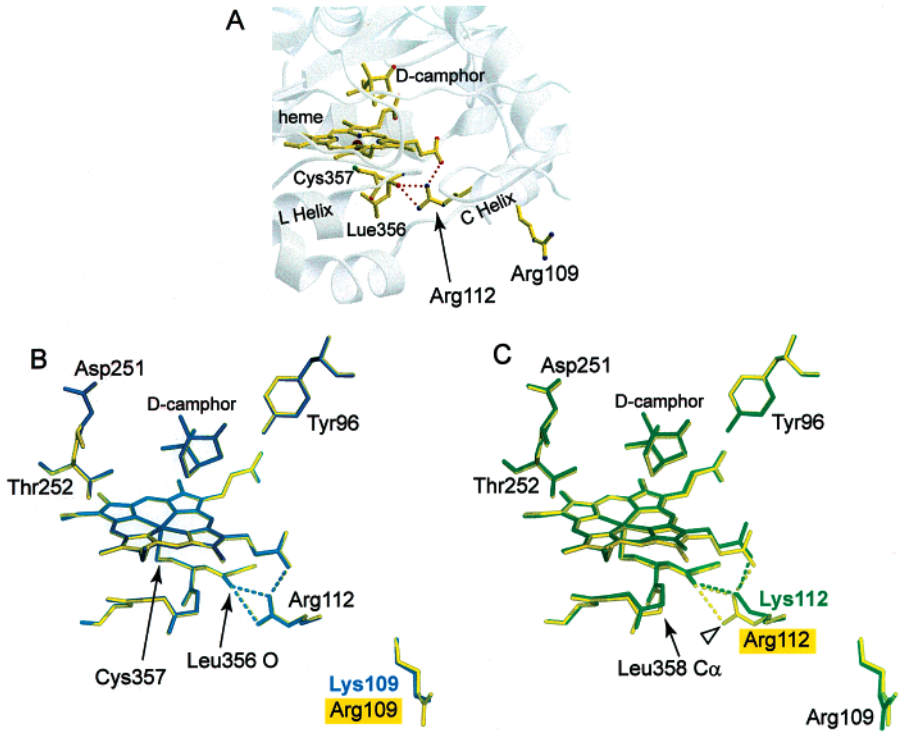

FIGURE 5: Crystal structures of ferric D-camphor-bound forms of P450cam. Panel A illustrates the active site and presumed Pdx-binding site of wild-type P450cam. The heme, D-camphor, the proximal ligand (Cys357), Leu356, Arg112, and Arg109 are shown in a yellow-colored stick model. Red, blue, brown, and green spheres represent oxygen, nitrogen, iron, and sulfur atom, respectively. Arg109 at the C helix extends toward the bulk water from the molecular surface, while Arg112 extends its side chain from the C helix toward the loop preceding the L helix forming hydrogen bonds (dashed line) with the heme 6-propionate and the main chain O atom of Leu356. Parts of the main chain are presented as a gray ribbon model. Panels B and C show the overlaid proximal side and the mutation site structures. Yellow, cyan, and green stick models show wild type, R109K, and R112K, respectively. The D-camphor, heme, main chain atoms of Leu356−Gln360, and side chains at 96, 109, 112, 251, and 252 are shown. The hydrogen bonds from Arg or Lys112 are drawn as dashed line. Open arrowhead indicates Arg112 Nη atom which is expected to hydrogen bond to Pdx. Figures were prepared by MOLSCRIPT (*40*) and RASTER3D (*41*) or PYMOL (*42*).

for the wild type, R109K, R112K, and R109Q, respectively, decreasing in the same order as in rates of decomposition (k_2) of oxyP450cam with reduced Pdx (Table 1). Furthermore, the oxy form of R112M, which does not decompose to products in the presence of a 200-fold excess of reduced Pdx over 500 ms, shows little spectral change when 20 equiv of reduced Pdx is added. These results indicate significant positive correlation between the conformational change and decomposition of the oxyP450cam/Pdx complex to products, implying that the conformational change promotes D-camphor hydroxylation by P450cam.

Enhanced Electron Donation from Proximal Ligand. ν_{C-O} and ν_{Fe-CO} can shift lower and higher, respectively, by increased back-donation from the heme iron (*30*). This inverse back-donation correlation is linear for the same proximal ligand to heme. According to the back-donation correlation of P450cam (*31*, *32*) together with 8 cm^{-1} downshift of ν_{C-O}, ν_{Fe-CO} is expected to upshift ca. 5 cm^{-1}. However, we have previously shown that ν_{Fe-CO} upshifts only 2 cm^{-1} upon Pdx binding (*33*), which is significantly smaller than the expected value. The small shift of ν_{Fe-CO} is explained in terms of enhanced electron donation from Cys ligand to the heme; the enhanced electron donation from a proximal ligand compete with σ-donation from the distal ligand, resulting in net lowering or smaller increase of ν_{Fe-CO} (*15*). Consistently, ν_{Fe-S} in ferric substrate-bound form upshifts ca. 3 cm^{-1} upon complexation with Pdx (*14*). Furthermore, NO-P450cam has two ν_{Fe-NO} bands and binding of reduced Pdx increases the intensity of the high-frequency band and decreases the low-frequency band, supporting the Pdx-binding induced increased electron donation from the proximal ligand, Cys357, to the heme iron (*15*). The enhanced electron donation from Cys357 would be caused by the alteration of the proximal side structure including Arg112 as discussed below.

Conformational Change Caused through Arg112. Arg112 extends its guanidium group to the loop preceding the L helix to form hydrogen bonds with heme propionate and the main chain carbonyl of Leu356 next to the proximal ligand. According to the model structure of the P450cam/Pdx complex reported by Pochapsky et al. (*16*), Arg112 hydrogen bonds to Pdx Asp38 that is located next to the redox center, a 2Fe-2S cluster. The critical role of the Asp38 for the interaction with P450cam is demonstrated by the lower affinity of the Asp38 → Asn mutant for P450cam (*34*). Thus, in the P450cam/Pdx complex, as we proposed previously (*35*), two metal centers interact with each other through the hydrogen bond network connected by the guanidium group of Arg112. In the R112K mutant, Lys112 is hydrogen bonded to the active center as found for Arg112 (Figure 5A,C). Although IR titration showed that R112K forms a 1:1 complex with Pdx and its overall structure was essentially unchanged, Lys112 would not be able to form a hydrogen bond with Pdx because its side chain N_ϵ atom is 2.7 Å closer to the active site (i.e., might be further away from Pdx) than the N_η of Arg112 which is expected to hydrogen bonds to

Pdx. Therefore, the amino acid substitution of Arg for Lys at 112 is expected to cause a loss or weakening of the interaction with Pdx through the side chain at 112. In fact, the mutation causes a decrease in the binding affinity toward reduced Pdx (Table 1). Furthermore, it is very interesting to note that the mutation significantly decreases the degree of the conformational change. Hence, a hydrogen bond network around Arg112 has a primary role in the conformational change. Such a role of Arg112 can also be envisaged in P450cam in the absence of Pdx as indicated by the different band II/band I ratio for wild type and 112 mutants (traces d and e in Figure 3B). On the other hand, the mutation of Arg109, which has no direct interaction with the proximal side of the heme, to Lys or Gln does not cause the conformational change in P450cam in the absence of Pdx but instead assists in the interaction between Pdx and P450cam via Arg112 by docking the two proteins in a proper orientation as shown by the limited conformational change of the 109 mutants upon Pdx binding. The 109 and 112 mutations thus alter the hydrogen bond network including Arg112, heme propionate, and proximal heme ligand, resulting in an increase in electron donation from Cys357. In fact, mutations at the proximal site, such as Leu358 → Pro and Gln360 → Leu or Pro significantly altered the hydrogen bond network around Cys357 and, subsequently, changed the electron donation properties of the proximal ligand (*36*).

As to the effects of Pdx binding on the structure of P450cam, we must also consider the previously proposed mechanism (*14*): electron donation is enhanced by shielding of positive charges by acidic residues of Pdx at the proximal face of P450cam. According to the mechanism, a mutation that removes surface positive charge is expected to cause a downshift of band I and/or increase in a ratio of band II/band I of CO-P450cam in the absence of Pdx. Contrary to this expectation, R109Q and R79Q showed neither downshift of band I nor increase of band II/band I ratio (spectrum for R79Q not shown). These results are not compatible with the mechanism, suggesting that shielding of positive charge is not a primary cause for the conformational conversion. These arguments again lead us to suggest that Pdx binding causes structural change around the proximal ligand through Arg112, resulting in changes of various spectroscopic properties including current IR data. Consistently, the R112K mutation, which altered the conformation of the proximal side loop including Cys356, increased the band II/band I ratio.

Significance on Oxygen Activation. Similar to the results obtained with CO-P450cam, an increase in a lower ν_{O-O} band and concomitant decreases in higher ν_{O-O} bands upon complexation with Pdx have been reported (*32*). Another similar spectral change is that the inverse correlation does not apply to ν_{Fe-XO}/ν_{X-O} (X = C or O) of both CO-P450cam and oxyP450cam. This unusual relationship would be explained by an enhanced electron donation from the proximal ligand and a σ-competition effect (*15*) as discussed above. These similar spectroscopic properties indicated that essentially the same conformational change is taking place upon Pdx binding irrespective of the ligand bound to ferrous P450cam. These arguments allow us to discuss how oxygen activation by P450cam is promoted by the conformational change.

As already mentioned, Pdx-binding changes the proximal side hydrogen bond network by interactions via Arg112, resulting in enhanced electron donation from the proximal ligand to the heme iron. The enhanced electron donation increases electron density in the dπ(Fe) orbital and the π-back-donation from the iron to O_2 ligand, which facilitates cleavage of O−O bond to give an active oxygen species, oxo-ferryl π-cation radical species called compound I. Similar enhancement of O−O bond scission is also observed for the mutant P450cam, L358P, which has shown to have stronger electron donation than wild type in the absence of Pdx (*36*, *37*).

It has recently been proposed that the Pdx binding induced conformational changes prevent uncoupling of oxygen consumption to the substrate hydroxylation by enforcing a conformation of P450cam that prevents loss of substrate and/or intermediates prior to turnover (*10*) or by relocation of D-camphor closer to the reactive oxygen atom of compound I (*11*). However, the 109 and 112 mutants, which all showed very limited conformational change, utilized almost all the oxygen consumed to hydroxylate D-camphor as wild type. Therefore, contrary to their proposal, IR detectable conformational change is not related with the coupling of dioxygen reduction to the substrate monooxygenation although the current data do not preclude the occurrence of the structural change at the distal site.

In the breakdown of oxyP450cam, electron transfer is one of the critical steps. It is possible that Pdx binding modulates the redox potentials of the two metal centers, thereby changing the electron-transfer rate. However, as already mentioned, two other iron−sulfur proteins, beef adrenodoxin and spinach ferredoxin, which have lower redox potentials than Pdx, cannot donate an electron to oxyP450cam to yield the reaction products (*8*). Therefore, it is less likely that the change of the redox potential induced by Pdx binding, if any, promotes breakdown of oxyP450cam. On the other hand, electronic coupling and/or reorganization energy, which are other critical parameters for electron-transfer rate, could be changed as follows.

We have already reported that EPR spectra of reduced Pdx also changed upon binding of CO-, NO-, or O_2-bound P450cam, suggesting that the structure around the 2Fe-2S cluster is changed by hexacoordinated P450cam binding (*35*). The 109 and 112 mutants, as found for IR spectroscopy, also show less spectral changes. Therefore, the conformation of intervening residues and, possibly, water molecule(s) (*38*) between the two metal centers changed simultaneously upon complex formation. It is of interest to note that the mutations at 112 drastically decelerate the electron transfer from reduced Pdx to ferric P450cam (*20*). It would thus be possible that the conformational change modulates an electronic coupling between the two metal centers as shown in Zn cytochrome *c*/plastcyanin complex (*39*) or reorganization energy to increase the electron-transfer rate.

Conclusions. We have found significant positive correlation between the Pdx-induced conformational change of CO-P450cam and the breakdown rates of oxyP450cam/Pdx complex to give the reaction products. Contrary to the previously proposed role of the conformational change, no significant relationship between the conformational change and the coupling ratio was observed. Pdx binding would modulate the conformation of the intervening residues between the two metal centers through Arg112, resulting in the enhancement of electron donation from the proximal

ligand to the heme iron and, possibly, electron transfer from Pdx to oxyP450cam to activate molecular oxygen.

The breakdown of oxyP450cam into the reaction products is a composite of several processes such as proton transfer, electron transfer, O−O bond cleavage, and oxygen transfer to the substrate. Thus, to fully understand the roles of the conformational changes on the P450cam monooxygenase system, further studies on the effects of Pdx on each partial reaction and on the structure of the oxyP450cam/Pdx complex are necessary.

ACKNOWLEDGMENT

The authors thank Prof. Thomas L. Poulos and Dr. Bhaskar for helpful comments and Ms. Yoko Toba for her excellent technical assistance.

REFERENCES

1. Katagiri, M., Ganguli, B. N., and Gunsalus, I. C. (1968) *J. Biol. Chem. 243*, 3543−3546.
2. Gunsalus, I. C., Meeks, J. R., Lipscomb, J. D., Debrunner, P., and Munck, E. (1974) in *Molecular Mechanisms of Oxygen Activation* (Hayaishi, O., Ed.) pp 559−613, Academic Press, New York.
3. Shimada, H., Sligar, S. G., Yoem, H., and Ishimura, Y. (1997) in *Oxygenase and Model System* (Funabiki, T., Ed.) pp 195−221, Kluwer Academic Publisher, London.
4. Kimata, Y., Shimada, H., Hirose, T., and Ishimura, Y. (1995) *Biochem. Biophys. Res. Commun. 208*, 96−102.
5. Hishiki, T., Shimada, H., Nagano, S., Egawa, T., Kanamori, Y., Makino, R., Park, S. Y., Adachi, S., Shiro, Y., and Ishimura, Y. (2000) *J. Biochem. (Tokyo) 128*, 965−974.
6. Gerber, N. C., and Sligar, S. G. (1994) *J. Biol. Chem. 269*, 4260−4266.
7. Gerber, N. C., and Sligar, S. G. (1992) *J. Am. Chem. Soc. 114*, 8742−8743.
8. Lipscomb, J. D., Sligar, S. G., Namtvedt, M. J., and Gunsalus, I. C. (1976) *J. Biol. Chem. 251*, 1116−1124.
9. Shiro, Y., Iizuka, T., Makino, R., Ishimura, Y., and Morishima, I. (1989) *J. Am. Chem. Soc. 111*, 7707−7711.
10. Pochapsky, S. S., Pochapsky, T. C., and Wei, J. W. (2003) *Biochemistry 42*, 5649−5656.
11. Tosha, T., Yoshioka, S., Takahashi, S., Ishimori, K., Shimada, H., and Morishima, I. (2003) *J. Biol. Chem. 278*, 39809−39821.
12. Lipscomb, J. D. (1980) *Biochemistry 19*, 3590−3599.
13. Ishimura, Y., Makino, R., Iizuka, T., and Shimada, H. (1987) in *Cytochrome P450: New Trends* (Sato, R., Omura, T., Imai, Y., and Fujii-Kuriyama, Y., Eds.) pp 151, Yamada Science Foundation, Nara.
14. Unno, M., Christian, J. F., Benson, D. E., Gerber, N. C., Sligar, S. G., and Champion, P. M. (1997) *J. Am. Chem. Soc. 119*, 6614−6620.
15. Unno, M., Christian, J. F., Sjodin, T., Benson, D. E., Macdonald, I. D., Sligar, S. G., and Champion, P. M. (2002) *J. Biol. Chem. 277*, 2547−2553.
16. Pochapsky, T. C., Lyons, T. A., Kazanis, S., Arakaki, T., and Ratnaswamy, G. (1996) *Biochimie 78*, 723−733.
17. Kramer, W., Drutsa, V., Jansen, H. W., Kramer, B., Pflugfelder, M., and Fritz, H. J. (1984) *Nucleic Acids Res. 12*, 9441−9456.
18. Imai, M., Shimada, H., Watanabe, Y., Matsushima-Hibiya, Y., Makino, R., Koga, H., Horiuchi, T., and Ishimura, Y. (1989) *Proc. Natl. Acad. Sci. U.S.A. 86*, 7823−7827.
19. Gunsalus, I. C., and Wagner, G. C. (1978) *Methods Enzymol. 52*, 166−188.
20. Unno, M., Shimada, H., Toba, Y., Makino, R., and Ishimura, Y. (1996) *J. Biol. Chem. 271*, 17869−17874.
21. Brewer, C. B., and Peterson, J. A. (1986) *Arch. Biochem. Biophys. 249*, 515−521.
22. Harris, T. K., Davidson, V. L., Chen, L., Mathews, F. S., and Xia, Z. X. (1994) *Biochemistry 33*, 12600−12608.
23. Schulze, H., Ristau, O., and Jung, C. (1994) *Eur. J. Biochem. 224*, 1047−1055.
24. Caughey, W. S., Shimada, H., Choc, M. G., and Tucker, M. P. (1981) *Proc. Natl. Acad. Sci. U.S.A. 78*, 2903−2907.
25. Poulos, T. L., Perez, M., and Wagner, G. C. (1982) *J. Biol. Chem. 257*, 10427−10429.
26. Koga, H., Sagara, Y., Yaoi, T., Tsujimura, M., Nakamura, K., Sekimizu, K., Makino, R., Shimada, H., Ishimura, Y., Yura, K., Go, M., Ikeguchi, M., and Horiuchi, T. (1993) *FEBS Lett. 331*, 109−113.
27. Nakamura, K., Horiuchi, T., Yasukochi, T., Sekimizu, K., Hara, T., and Sagara, Y. (1994) *Biochim. Biophys. Acta 1207*, 40−48.
28. Jung, C., Hoa, G. H., Schroder, K. L., Simon, M., and Doucet, J. P. (1992) *Biochemistry 31*, 12855−12862.
29. O'Keefe, D. H., Ebel, R. E., Peterson, J. A., Maxwell, J. C., and Caughey, W. S. (1978) *Biochemistry 17*, 5845−5852.
30. Ray, G. B., Li, X. Y., Ibers, J. A., Sessler, J. L., and Spiro, T. G. (1994) *J. Am. Chem. Soc. 116*, 162−172.
31. Legrand, N., Bondon, A., Simonneaux, G., Jung, C., and Gill, E. (1995) *FEBS Lett. 364*, 152−156.
32. Sjodin, T., Christian, J. F., Macdonald, I. D., Davydov, R., Unno, M., Sligar, S. G., Hoffman, B. M., and Champion, P. M. (2001) *Biochemistry 40*, 6852−6859.
33. Makino, R., Iizuka, T., Ishimura, Y., Uno, T., Nishimura, Y., and Tsuboi, M. (1984) in *Ninth International Conference on Raman Spectroscopy*, pp 492−493, Chemical Society of Japan, Tokyo.
34. Holden, M., Mayhew, M., Bunk, D., Roitberg, A., and Vilker, V. (1997) *J. Biol. Chem. 272*, 21720−21725.
35. Shimada, H., Nagano, S., Ariga, Y., Unno, M., Egawa, T., Hishiki, T., Ishimura, Y., Masuya, F., Obata, T., and Hori, H. (1999) *J. Biol. Chem. 274*, 9363−9369.
36. Yoshioka, S., Tosha, T., Takahashi, S., Ishimori, K., Hori, H., and Morishima, I. (2002) *J. Am. Chem. Soc. 124*, 14571−14579.
37. Yoshioka, S., Takahashi, S., Ishimori, K., and Morishima, I. (2000) *J. Inorg. Biochem. 81*, 141−151.
38. Furukawa, Y., and Morishima, I. (2001) *J. Biol. Chem. 276*, 12983−12990.
39. Ivkovic-Jensen, M. M., and Kostic, N. M. (1996) *Biochemistry 35*, 15095−15106.
40. Kraulis, P. J. (1991) *J. Appl. Crystallogr. 24*, 946−950.
41. Merritt, E. A., and Murphy, M. E. P. (1994) *Acta Crystallogr. D 50*, 869−873.
42. DeLano, W. L. (2002), DeLano Scientific, San Carlos, CA.

BI035410P